

# Detonation Initiation, Propagation, and Structural Response

J. E. Shepherd, J. Austin, T. Chao, F. Pintgen, E. Wintenberger, S. Jackson, M. Cooper  
*Graduate Aeronautical Laboratories, California Institute of Technology*  
*Pasadena, CA 91125 USA*

**Research at Caltech is being carried out into the reaction zone structure of a propagating detonation, the initiation of detonation using shock and detonation focusing, direct measurement of impulse in single detonation and DDT events for storable fuels, the measurement of vapor pressure and detonation cell width for such fuels, and the structural response of detonation tubes, including fracture and failure.**

## Introduction

The Explosion Dynamics Laboratory research group at Caltech is carrying out investigations on many aspects of detonation initiation and propagation which are relevant to pulse detonation engines. A brief review of these activities is presented here.

## PLIF Imaging

Direct experimental observations<sup>1</sup> of the reaction zone structure in propagating detonations have been made using planar laser induced fluorescence (PLIF) of the OH radical. For the first time, images were obtained with sufficient spatial resolution to resolve 'keystone' features in the reaction front due to variations in the lead shock strength.

Experiments were carried out in the 150x150 mm test section of the detonation tube at Caltech. OH molecules were excited using an excimer-pumped dye laser tuned to 284.008 nm, halfway between the transitions (1,0) Q<sub>2</sub>(8) and (1,0) Q<sub>1</sub>(9). An 80 x 0.3 mm planar light sheet was formed and entered the test section through a quartz window in the end flange. The induced fluorescence, filtered with a 313 nm filter (10 nm FWHM), was collected by an ICCD camera positioned at 90° to the direction of propagation of the detonation, visualizing a cross-section of the flow. Experiments performed with a partially blocked laser light sheet confirmed that the natural chemiluminescence in the images was negligible. Some simultaneous Schlieren images were obtained. Stoichiometric hydrogen-oxygen mixtures at 20 kPa were studied with different diluents to examine the effect of cell regularity on reaction zone structure.

Keystone structures were observed for all mixtures. Mixtures with argon dilution showed much more regular structure than mixtures diluted with nitrogen. Shock and detonation polar analysis was used in the vicinity of the triple point to determine that the keystones are bounded by the reaction zones behind the incident wave and Mach stem and by the shear layer.

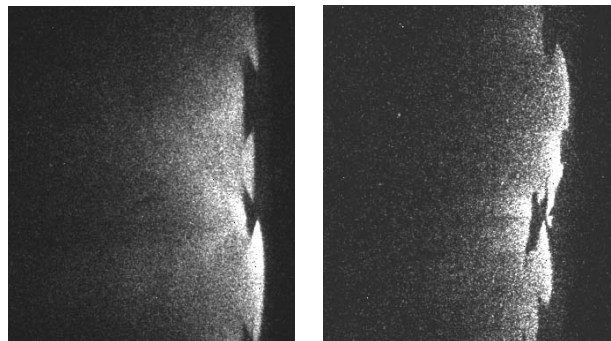


Figure 1. OH PLIF images of reaction zone structure in propagating detonations revealing 'keystone' features. On the left, the hydrogen-oxygen mixture is diluted with argon (85%), on the right with nitrogen (60%). Wave propagation is from left to right.

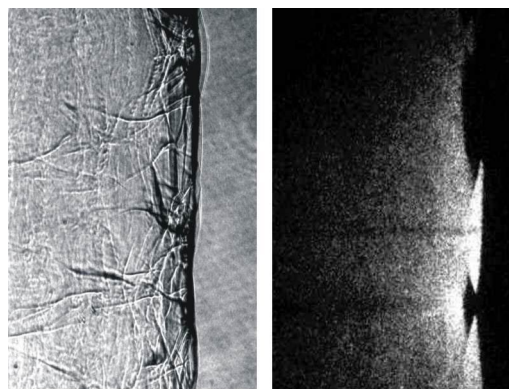


Figure 2. Simultaneous Schlieren and PLIF images of detonation structure.

To obtain a full description of the detonation structure, it is necessary to visualize both the chemical reaction zone and the shock waves. Simultaneous PLIF and Schlieren images are shown above. While the PLIF technique images only a cross-section of the flow, the Schlieren image is integrated through the volume of the test section, resulting in superposition of the shock structures. In order to reduce the shock geometry to two dimensions, a new facility is being designed. Preliminary experiments aimed at determining suitable

facility dimensions have been completed. A further application of the work is in understanding the coupling between shocks and chemical reaction that occur in detonation initiation.

### JP10 Cell Width Measurement

Liquid fuels with high energy density are desirable for pulse detonation engines. Cell width data provide a measure of the detonability of such fuels. Cell width measurements were carried out for JP10 ( $C_{10}H_{16}$ ) in the Caltech 280-mm detonation tube at elevated temperatures (80 -100 °C) with pure vapor phase fuel in order to avoid problems connected with dispersing and characterizing sprays. To ensure the fuel had fully vaporized and the mixture composition was known, the temperature was monitored at 19 locations in the tube and in the circulation lines. The partial pressure of the fuel vapor was recorded and compared to vapor pressure data obtained at Caltech (see discussion below). Wave speed measurements were made for comparison with the calculated CJ velocity. Mixtures were initiated directly by an exploding wire in a short section of acetylene-oxygen mixture.

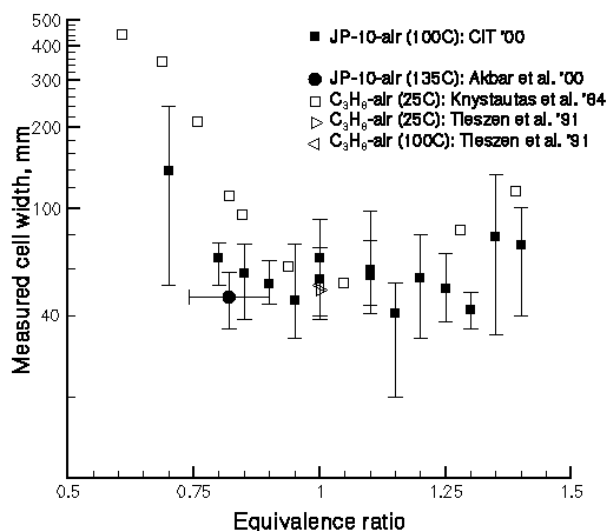


Figure 3. Detonation cell width measurements in JP10-air mixtures with varying stoichiometry. Previous results<sup>2,3,4</sup> for JP10- and propane-air are given for comparison.

Fuel-oxygen mixtures with varying nitrogen dilution, up to an amount corresponding to a fuel-air mixture, stoichiometry, and initial pressure were studied.

Our study shows that the cell width of JP10 is very similar to that of propane, indicating that propane may be a useful surrogate for initial investigations.

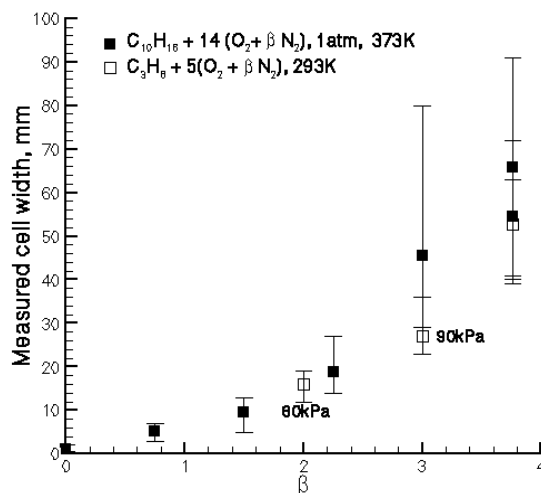


Figure 4. Cell width measurements in JP10-O<sub>2</sub> with varying nitrogen dilution, where  $\beta$  is the ratio of N<sub>2</sub> to O<sub>2</sub> concentrations.

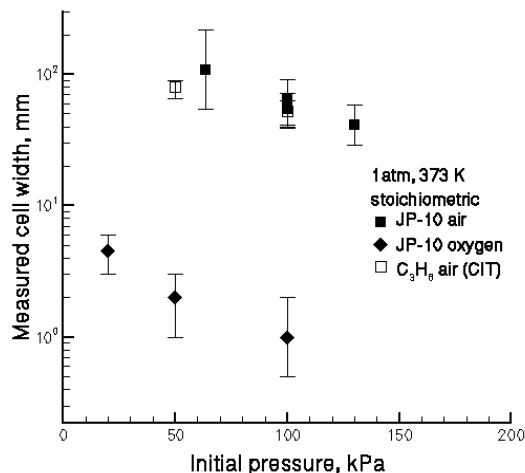


Figure 5. Cell width measurements in JP10 with varying initial pressure.

### JP-10-O<sub>2</sub>-N<sub>2</sub> & Propane-Air Detonations

The ability to detonate liquid hydrocarbon fuels is a critical issue associated with pulse detonation engines. Recent progress has been made in obtaining impulse measurements with propane and JP10, which have comparable cell sizes, for a range of nitrogen dilutions at 1 atm. The impulse was determined<sup>5</sup> by

measuring the displacement of a ballistic pendulum in which the detonation tube, initially filled with combustible gases, was suspended from the ceiling by steel wires. The combustion products were free to expand out from the tube into the surrounding large room. The detonation tube ( $L = 1.016$  m,  $d = 76.2$  mm) contained ten ionization gauges, three pressure transducers, and a spark plug as the ignition source. For propane and JP10 mixtures, the spark energy alone is not sufficient for transition to detonation within the tube. Thus, a separate ignition system utilizing an 'initiator', or driver with a more sensitive mixture of gases, was developed.

The ignition system consists of two main sections: a) separate reservoirs for the fuel and oxidizer, and b) steel initiation tube ( $L = 30.5$  cm,  $d = 2.54$  cm) containing a Shchelkin spiral. Each reservoir was separated from the initiation tube by a solenoid valve, which was calibrated to determine the relationship between valve duration, reservoir pressure, and percent of total (ignition system and main detonation tube) volume filled. The spark plug was located in the upstream flange of the initiation tube.

After introduction of the driver gases into the initiation tube, the spark starts a flame and the Shchelkin spiral causes transition to detonation resulting in a detonation at the end of the initiation tube. This detonation wave enters the main detonation chamber by diffracting around a blockage plate centered at the entrance of the tube. The imploding detonation wave generates a region of energy density sufficient to quickly initiate detonation in the main mixture.

Propane was initially tested to verify operation and compare with previous results. The driver gases were propane-oxygen at reservoir pressures that filled 2.2% of the total volume. The main detonation tube contained propane-oxygen-nitrogen test mixtures. The results appear in Figure 6. The specific impulse values were calculated by dividing the ballistic impulse,  $I$ , with the initial density,  $\rho$ , of the driver gases and test gas mixture, the total volume,  $V$ , and the gravitational acceleration,  $g$ .

A detonation was not initiated in propane-air with the driver filling 2.2% of the total volume. However, increasing the reservoir pressures so that 6% of the volume was filled with initiator mixture did result in a detonation.

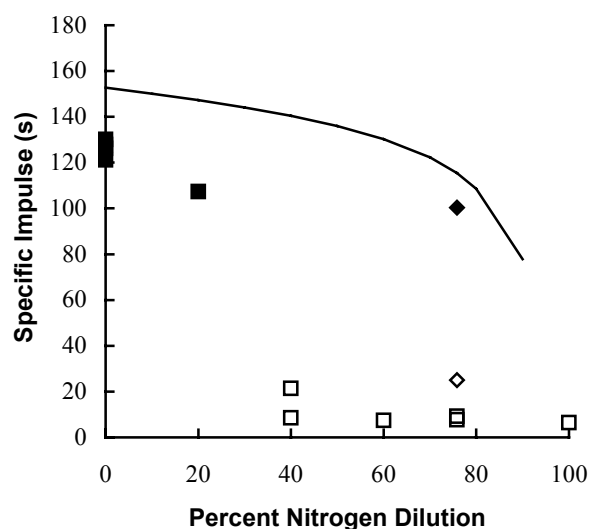


Figure 6. Ballistic impulse measurements in  $C_3H_8-O_2$  with nitrogen dilution, where specific impulse,  $I_{sp} = I/\rho Vg$ . Squares represent 2.2% driver volume and diamonds 6% driver volume, both at 295K. Open symbols are cases which did not detonate. In the experiment represented by the open diamond, the driver was heated to 373K. The theoretical prediction<sup>6</sup> is shown as a line.

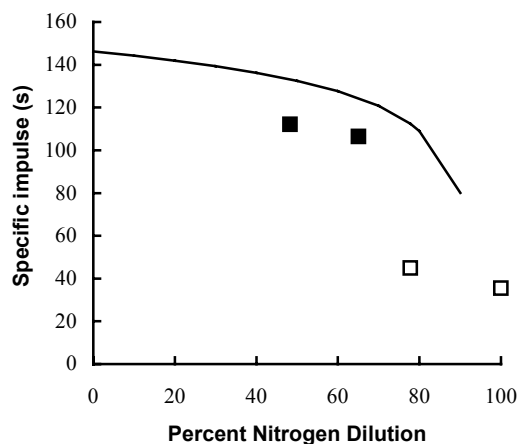


Figure 7. Ballistic impulse measurements in  $JP10-O_2$  with nitrogen dilution. Open symbols are cases which did not detonate. In all cases, the driver was  $C_2H_2-O_2$  (10% of the tube volume). The theoretical prediction<sup>6</sup> is shown as a line.

To obtain impulse measurements for JP10-oxygen-nitrogen test gas mixtures, the entire system was heated to 80 °C to vaporize the liquid JP-10. Heating the

tube and reservoirs decreased the effectiveness of the initiator such that a detonation in propane-air was no longer achieved when 6% of the total volume was filled with driver gases. Thus, the reservoirs were filled to a higher pressure with acetylene-oxygen (resulting in 10% of the total volume filled with driver gas). The impulse results appear in Figure 7. A detonation in JP10-air was not obtained, indicating a stronger ignition source is required.

### JP-10 Vapor Pressure Measurement

JP10 vapor pressure measurements were carried out to obtain reliable data for use in JP10 detonation experiments. The experimental facility was similar to that used in previous<sup>7</sup> vapor pressure measurements in Jet-A. A vessel containing liquid JP10 was placed in an ethylene glycol bath. The ethylene glycol was contained in a recipient enclosed in a heating system. Thorough mixing of the ethylene glycol and insulation of the recipient ensured uniform heating of the bath. The temperature was set using a digital controller and measured using thermocouples in the bath and in the test liquid. The temperature was varied from ambient to 120°C.

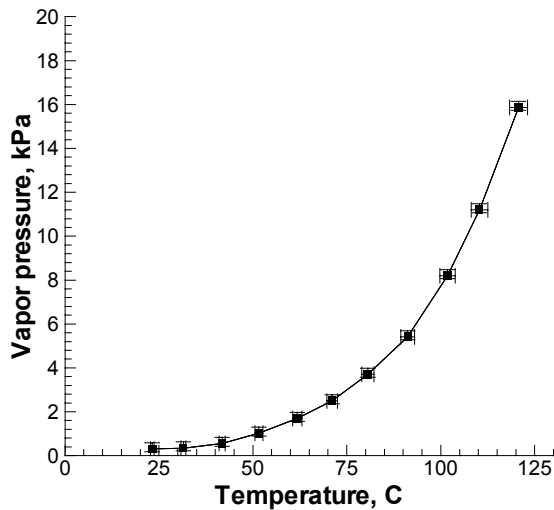


Figure 8. Vapor pressure measurements of JP10.

The vapor pressure of JP10 was measured in steps of 10°C using a digital pressure gauge. At every step, pressure measurements were taken only after ensuring that the temperature of the bath and the test liquid were stable. The gas into the vessel was then evacuated to minimize leak rate effects and the pressure started to build up again until it reached a constant value

corresponding to the vapor pressure. The results are plotted on Figure 8. The error bars represent the uncertainties in the measurements, which are  $\pm 2\%$  for the temperature and  $-0.13/+0.28$  kPa for the measured pressure, accounting for gauge precision and leak rate.

### Initiation By Detonation Focusing

We are currently working on methods of initiating detonations in less sensitive fuel-air mixtures (such as JP10 and air, or propane and air) that do not involve high energy input. Such methods are appealing for actual air-breathing aircraft applications since JP10 is a liquid fuel and air is readily available from the atmosphere.

One such method involves shock wave focusing. In shock wave focusing, two or more shock waves collide. In the region behind the colliding shock waves, high pressures and temperatures occur. In general, increased temperatures and pressures facilitate the initiation of detonation waves. There are two aspects of shock wave focusing that we are investigating. First, we are examining the characteristics of the focal region in order to develop criteria for the initiation of detonations under these conditions. Second, we are developing and testing practical devices that can be used for generating focused shock or detonation waves.

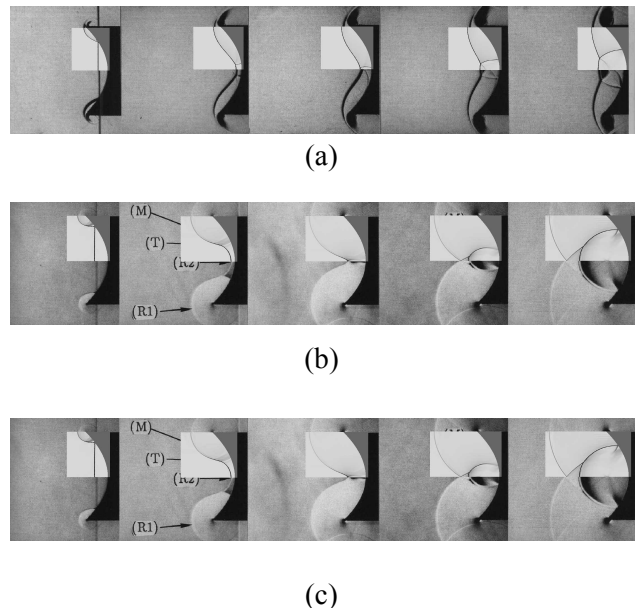


Figure 9. Numerical simulations of shock wave focusing using Amrita<sup>8</sup> and comparisons with previous experimental results of Izumi et al<sup>9</sup>.

A preliminary study has been performed by using numerical simulation to examine shock focusing in nonreactive mixtures and making comparisons with previous results. The results of several simulations are shown in Figure 9. Pressure and temperature amplifications were found to be very sensitive to the type of reflection. The type of reflection was determined as a function of the incident wave strength and the geometry. Three types of reflection are observed. Type A reflection is characterized by the formation at focusing of a strong Mach stem growing with time, leaving an open focal region. This reflection type occurs for strong shocks and shallow reflectors. Type B reflection happens when the diffracted shocks at the reflector edges intersect on the axis after focusing and then precede the Mach stem. Type C reflection happens when the diffracted shocks at the reflector edges intersect on the axis before focusing. It results in a closed focal region. It is characterized by a small triangular region of fluid being compressed at focusing. This reflection type is characteristic of weak shock waves and deep reflectors. A summary of the reflection regimes is given in Figure 10.

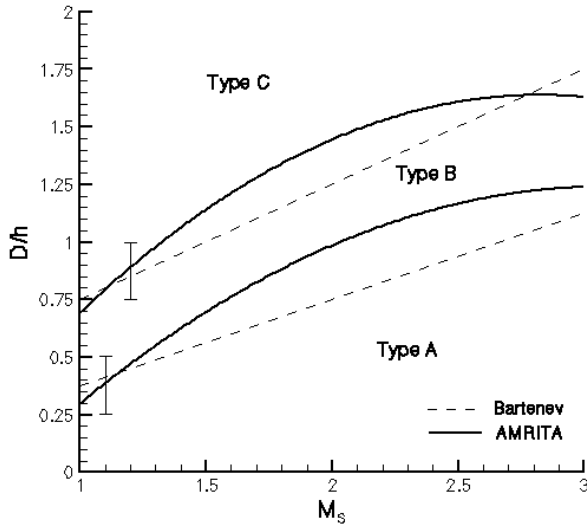


Figure 10. Map of focusing regimes as a function of reflector geometric parameters ( $D/h$  is the depth-to-half-height ratio) and incident shock Mach number  $M_s$ . Comparison between CFD (Amrita<sup>8</sup>) and previous studies (Bartenev et al.<sup>10</sup>).

Based on these simulations and previous experimental studies, we are designing experiments that will be carried out in the GALCIT 6-in shock tube. A test section for the shock tube is currently being

designed that will enable two-dimensional studies of the shock focusing process in combustible mixtures.

We have also developed a practical design for creating a focal region inside of a detonation tube without blocking the flow path and causing associated losses in propulsive efficiency. Our device is based on using an array of small diameter channels to generate and merge many detonation waves to create a single detonation wave with a toroidal front. A planar version of this device has been successfully built and tested<sup>11</sup> to demonstrate the principles of wave front merging to create a single front. We anticipate that the imploding toroidal shock wave will be highly effective at initiating detonations with virtually no initiator interference.

### Fracture experiments and correlations

Fracture response of thin-walled and pre-flawed tubes to single cycle detonation loads is being investigated to determine what constitutes a critical flaw. Preliminary data have shown the possibility of a fracture threshold behavior (Figure 11) that will be of important interest to pulse detonation engine structural designers. The fracture threshold divides a non-dimensional parameterized space into rupture and no-rupture regions.

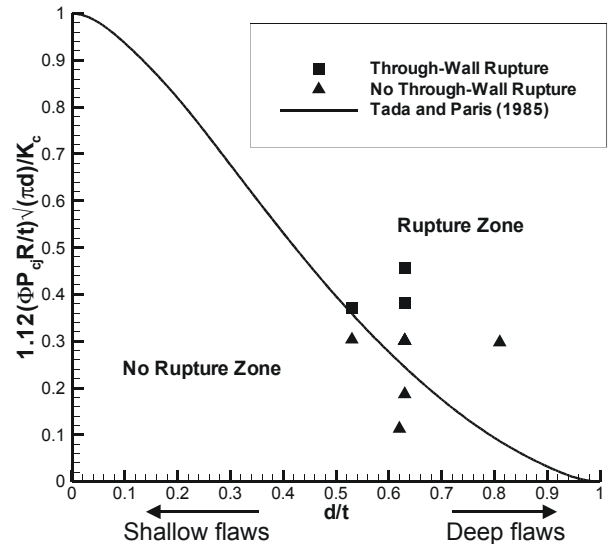


Figure 11. Developing fracture threshold of thin-walled and pre-flawed tubes under single cycle detonation loads with some preliminary data. Squares represent ruptured tubes; triangles are unruptured tubes. The model is an adaptation of static linear elastic fracture mechanics. It is expected to be invalid for very shallow or very deep flaws.

Parameters considered include Chapman-Jouguet detonation pressure,  $P_{CJ}$ , tube geometry (radius,  $R$ , to wall thickness,  $t$ , ratio), flaw geometry (flaw depth,  $d$ , to wall thickness ratio), dynamic amplification factor,  $\phi$ , and fracture toughness,  $K_{IC}$ .

The twenty experiments done so far with aluminum have indicated that the fracture threshold is more sensitive to flaw depth than flaw length. Future work will be to further refine this threshold by carrying out more experiments. The ultimate goal is to develop design guidelines<sup>12</sup> for minimum weight and maximum service life detonation tubes. Using a fracture-based design is particularly critical for some advanced materials under consideration for PDEs such as ceramics that are brittle but have high temperature endurance.

PDE materials will experience fatigue due to the traveling, repetitive, and thermal-mechanically impulsive loads. Fatigue crack growth will be a function of the amplitudes of the stress waves and the geometry of the flaw.

However, before attempts are made to measure the dynamic stresses in a fatigue-flawed multi-cycle pulse detonation tube, it is important to first understand the simpler problem of how the stress waves propagate in a flawed tube under single-cycle loads. Some of our future experiments will use strain gauges mounted on the surface of a flawed tube to monitor the dynamic stress concentrations around the flaw. In some experiments, the tubes will be deliberately ruptured so that the strains can be studied for different modes of dynamic fracture behavior such as crack spiraling and crack branching.

## References

<sup>1</sup>Pintgen, F., Eckett, C., Austin, J.M., Shepherd, J.E., "Direct observations of reaction zone structure in propagating detonations", to be presented at 18<sup>th</sup> ICDERS meeting, Seattle, 2001

<sup>2</sup>Akbar, R., Thibault, P.A., Harris, P.G., Lussier, L.-S. Zhang, F., Murray, S.B., Gerrard, K., "Detonation properties of unsensitized and sensitized JP-10 and Jet-A fuels in air for pulse detonation engines," AIAA-2000-3592

<sup>3</sup>Knystautas, R., Guirao, C., Lee, J.H.S., Sulmistras, A., "Measurement of cell size in hydrocarbon-air mixtures and predictions of critical tube diameter, critical

initiation energy and detonation limits", In Prog. Astronaut. Aeronaut., 94, :23-37, 1984

<sup>4</sup>Tieszen, S.R., Stamps, D.W., Westbrook, C.K., Pitz, W.J., "Gaseous hydrocarbon-air detonations", Combust. Flame, 84 (3):376-390, 1991

<sup>5</sup>Cooper, M., Jackson, S., Austin, J.M., Wintenberger, E., and Shepherd, J.E., "Direct experimental impulse measurements for detonations and deflagrations", AIAA paper 2001-3812

<sup>6</sup>Wintenberger, E., Austin, J.M., Cooper, M., Jackson, S., Shepherd, J.E., "An analytical model for the impulse of a single-cycle pulse detonation engine", AIAA 2001-3811, 2001

<sup>7</sup>Shepherd, J.E., Nuyt, C.D., Lee, J.J., "Flash Point and Chemical Composition of Aviation Kerosene (Jet A)". Explosion Dynamics Laboratory Report FM99-4, California Institute of Technology, December 1999

<sup>8</sup>Quirk, J.J., "Amrita: A computational facility (for CFD modeling)". In 29<sup>th</sup> Computational Fluid Dynamics Lecture Series, Von Karman Institute, 1998

<sup>9</sup>Izumi, K., Aso, S., Nishida, M., "Experimental and computational studies of focusing processes in shock waves reflected from parabolic reflectors," Shock Waves 3, 341-345, 1994.

<sup>10</sup>Bartenev, A.M., Khomik, B.E., Gelfand, B.E., Gronig, H., Olivier, H., "Effect of reflection type on detonation initiation at shock wave focusing," Shock Waves 10, 197-204, 2000.

<sup>11</sup>Jackson, S.I., Shepherd, J.E., "A planar detonation initiator", to be presented at 18<sup>th</sup> ICDERS meeting, Seattle, 2001

<sup>12</sup>Chao, T., Wintenberger, E., Shepherd, J.E., "On the design of pulse detonation engines", GALCIT report FM00-7, California Institute of Technology, 2000